UC-403
LBL-28601

Lawrence Berkeley Laboratory
UNIVERSITY OF CALIFORNIA

EARTH SCIENCES DIVISION

To be presented at the International Conference
on Rock Joints, Loen, Norway, June 4–6, 1990,
and to be published in the Proceedings

Hydromechanical Coupling Between Stress, Stiffness, and Hydraulic Conductivity of Rock Joints and Fractures

R.W. Zimmerman, D.W. Chen, J.C.S. Long, and N.G.W. Cook

February 1990

For Reference

Not to be taken from this room

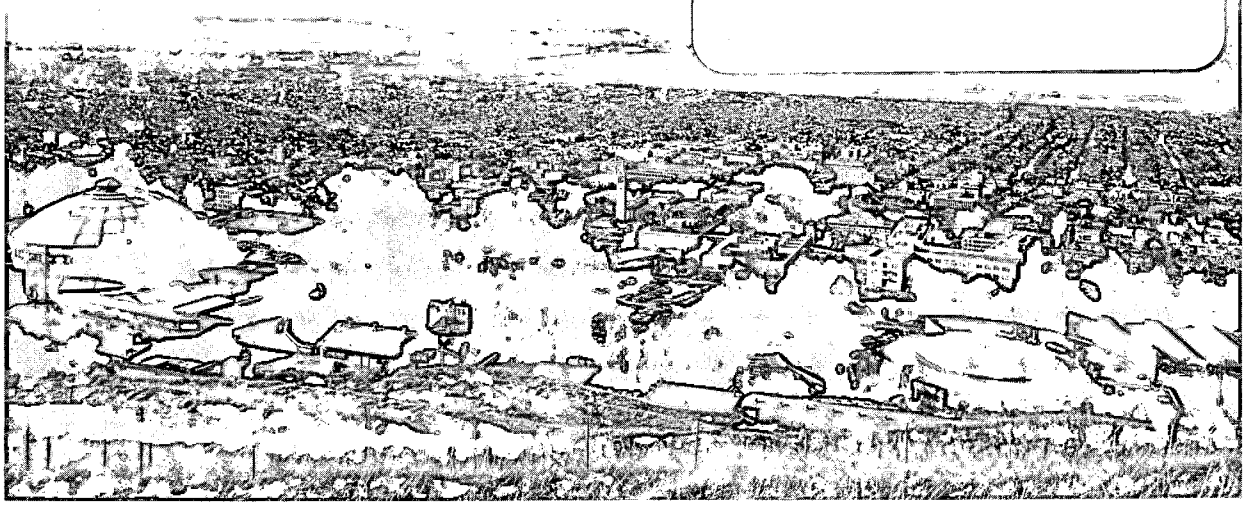

LBL-28601
Copy 1
Bldg. 50 Library.

Prepared for the U.S. Department of Energy under Contract Number DE-AC03-76SF00098.

DISCLAIMER

This document was prepared as an account of work sponsored by the United States Government. While this document is believed to contain correct information, neither the United States Government nor any agency thereof, nor the Regents of the University of California, nor any of their employees, makes any warranty, express or implied, or assumes any legal responsibility for the accuracy, completeness, or usefulness of any information, apparatus, product, or process disclosed, or represents that its use would not infringe privately owned rights. Reference herein to any specific commercial product, process, or service by its trade name, trademark, manufacturer, or otherwise, does not necessarily constitute or imply its endorsement, recommendation, or favoring by the United States Government or any agency thereof, or the Regents of the University of California. The views and opinions of authors expressed herein do not necessarily state or reflect those of the United States Government or any agency thereof or the Regents of the University of California.

LBL-28601

Hydromechanical Coupling Between Stress, Stiffness, and Hydraulic Conductivity of Rock Joints and Fractures

*R. W. Zimmerman, D. W. Chen, J. C. S. Long, and N. G. W. Cook**

Earth Sciences Division
Lawrence Berkeley Laboratory
University of California
Berkeley, California 94720

and

*Department of Materials Science and Mineral Engineering
University of California

February 1990

This work was supported by the Manager, Chicago Operations, Repository Technology Program, Repository Technology and Transportation Division, and by the Director, Office of Energy Research, Office of Basic Energy Sciences, Engineering and Geosciences Division, of the U.S. Department of Energy under Contract No. DE-AC03-76SF00098.

Hydromechanical Coupling Between Stress, Stiffness, and Hydraulic Conductivity of Rock Joints and Fractures

*R.W. Zimmerman, D.W. Chen, J.C.S. Long, and N.G.W. Cook**

Earth Sciences Division
Lawrence Berkeley Laboratory
University of California
Berkeley, CA 94720

*Dept. of Materials Science and Mineral Engineering
University of California
Berkeley, CA 94720

ABSTRACT

The mechanical stiffness and hydraulic conductivity of simulated fractures are studied as a function of normal stress. Simulated fractures are created by discretizing the fracture plane into a square array, and randomly assigning an aperture to each square according to some statistical law. The mechanical deformation of the fracture is computed with a three-dimensional elastostatic boundary element method, while the fluid flow problem is reduced to a two-dimensional Laplace equation, which is also solved with a boundary element method. This method allows a study of the effect of various statistical parameters of the aperture distribution on the hydromechanical properties of fractures.

To be presented at the ISRM International Conference on Rock Joints, Loen, Norway, 4-6 June 1990

1. INTRODUCTION

The hydraulic and mechanical behavior of a rock fracture or joint is strongly dependent on the geometry of the void space. Although fractures are usually considered to be nominally planar features, they actually consist of isolated asperity regions where the two rock surfaces are in contact, surrounded by regions where the two surfaces are separated by an aperture, h. Although they are sometimes modeled as being circular (Walsh 1981) or elliptical (Chen et al. 1989), the asperity regions of real fractures are usually irregular in shape (Hopkins et al. 1987). And while the aperture is often assumed to be constant from point to point, it in fact typically varies in an irregular manner. We can consider a rock fracture to be composed of two irregular surfaces in partial contact (Brown & Scholz 1985).

When fluid flows through such a fracture, it flows through those channels that have the largest apertures, and around the contact areas. Hydraulic conductance is locally proportional to the cube of the aperture (Brown 1987), so the permeability depends on the amount of contact area, the spatial distribution of the contact areas, as well as the aperture height (Chen et al. 1989). All of these parameters are, in turn, functions of the stress to which the fracture is subjected. As the normal stress acting on a fracture increases, the apertures will decrease. In some parts of the fracture, this deformation will be large enough that new contact areas are created (Tsang & Witherspoon 1981). Both of these effects, the decrease of the aperture and the creation of new contact area, will cause the permeability to decrease.

The mechanical stiffness of a fracture also depends on the geometry of the fracture, as well as on the mechanical properties of the intact rock. It is to be expected that the stiffness will increase as the area of contact increases, since a fracture without any contact regions would possess no stiffness whatsoever. It is also true, although it is perhaps not obvious, that the stiffness will depend on the size and shape of the contact areas, aside from its dependence on the amount of contact area (Hopkins et al. 1987). For any given distribution of contact areas, the stiffness does not depend explicitly on the aperture; this is analogous to the fact that, to a very high approximation, the increase in the compressibility of a rock due to a penny-shaped crack is independent of the aperture of the crack (Zimmerman et al. 1986). However, the aperture does determine the rate at which new contact area is created under the application of a normal

load. Hence, the stress-dependence of stiffness will be strongly influenced by the distribution of apertures.

We have attempted to model the phenomena described above, using boundary element methods (Brebbia 1978; Crouch & Starfield 1983). These are a class of numerical methods in which numerical discretization and calculation is needed only along the boundary of the region of interest. This reduces the dimensionality of the problem by one, thereby allowing a great reduction in the size of the matrix equations that must be solved. The stiffness of the fracture is modeled in terms of the deformation of a half-space that is subjected to normal loads across the "contact areas". This necessitates the solution of the full three-dimensional equations of elasticity for the infinite half-space. The flow problem should in principle be modeled by the three-dimensional Navier-Stokes equations for incompressible viscous flow. However, since the full Navier-Stokes equations are difficult and time-consuming to solve, we have modeled the fluid flow problem in the fractures with the lower-order Laplace equation, which neglects velocity components normal to the fracture plane. (This replacement procedure will be described in more detail below.) The advantage of our approach is that both the mechanical deformation and permeability of a fracture can be studied using the same fracture geometry for both problems. In this way we are able to study the effect of the aperture distribution, and the distribution of contact areas, on both stiffness and permeability (cf., Barton et al. 1985; Pyrak-Nolte et al. 1987).

2. FORMULATION OF THE STIFFNESS PROBLEM

For the purposes of finding the normal stiffness of the fracture, we assume that the fracture is composed of two symmetric rough surfaces in contact. Because of symmetry, we need only to solve the equations of elastic equilibrium in one of the semi-infinite half-spaces that are bounded by the fracture. If the amplitude of the roughness is small enough, the boundary conditions on the half-space can be assumed to act along the nominally flat "plane" of the fracture. In the absence of body forces, the equations of elastic equilibrium are (Sokolnikoff 1956)

$$(1-2\nu)\nabla^2\vec{u}(x,y,z) + \nabla:\nabla\vec{u}(x,y,z) = 0 \ , \qquad (1)$$

where the plane $z = 0$ is the fracture plane, and ν is Poisson's ratio. The stresses and displacements are assumed to vanish as $x^2+y^2 \to \infty$. Along the $z=0$ boundary, the proper boundary conditions depend on whether or not the point (x,y,0) is a region of contact between the two faces of the fracture. If the faces are in contact, we use the conditions that

$$\sigma_{zx} = \sigma_{zy} = 0, \quad u_z = 0 . \tag{2}$$

The no-shear boundary conditions assume that the rock faces are frictionless; the calculations can also be carried out under the "opposite" assumption, which is that no shear displacements are allowed, i.e., $u_x = u_y = 0$. At points where the faces are not in contact, the boundary conditions are

$$\sigma_{zx} = \sigma_{zy} = 0, \quad \sigma_{zz} = -T_{zz}, \tag{3}$$

where T_{zz} is the normal traction.

The basic ingredient in the boundary element method that we use to solve eqs. (1-3) is the "displacement discontinuity" source. This is a "point source" that represents a discontinuity D_i in the displacements, across the plane $z=0$, i.e.,

$$D_i = u_i(x,y,z=0^-) - u_i(x,y,z=0^+) . \tag{4}$$

The components of the fundamental solution that corresponds to displacement discontinuities in the three orthogonal directions have been found by Rongved (1957), but are too lengthy to be reprinted here. These solutions give the displacements and stresses at an arbitrary point (ζ,η,ξ), due to a displacement discontinuity at a point (x,y,z).

In order to solve the elasticity equations using the boundary element method, we first discretize the $z=0$ plane into a rectangular grid of $M \times N$ square elements. Each element is assumed to be small enough so that the normal stress σ_{zz} can be assumed constant across it. A point source of displacement discontinuity, with unknown magnitude, is then assumed to act at the center of each element. If we write down the

displacements and stresses at each element along the boundary, in terms of the unknown magnitudes of these point sources, we arrive at a set of $3 \times M \times N$ linear equations, which can be solved numerically. Once the magnitudes of the sources are found, we can calculate the displacement of the fracture walls.

3. FORMULATION OF THE FLOW PROBLEM

The flow of a Newtonian fluid through a rock fracture is governed by the Navier-Stokes equations of fluid mechanics (Batchelor 1967). Exact solutions to these equations can be obtained for very simple geometries, such as the "parallel plate" model of a fracture (Tsang & Witherspoon 1981). For somewhat more realistic geometries, such as two smooth, parallel fracture walls propped open by circular columns that are intended to represent the asperities, approximate solutions of the Navier-Stokes equations are feasible (Kumar et al. 1989). For models that take into account the irregularity of real fracture surfaces, however, analytic solutions are not obtainable. Unfortunately, numerical solution of the full three-dimensional Navier-Stokes equations is far from trivial.

In order to circumvent this difficulty, we have only performed flow simulations under the assumption that the aperture, in those regions not obstructed by asperities, is equal to a constant, h. We therefore sacrifice some of the effect of aperture variation, while still accounting for the effect of contact area and of the effect of the mean aperture, which still varies with stress. For this model, subject to a few other conditions, the Navier-Stokes equations can be reduced to a Laplace equation. One necessary condition for this simplification is that the flow rate must be sufficiently low, as measured by the reduced Reynolds' number. Specifically, this requires that (Schlichting 1968)

$$Re^* = \frac{\rho U h^2}{\mu L} \ll 1 , \tag{5}$$

where ρ is the fluid density, U is the mean velocity, μ is the fluid viscosity, and L is the typical distance between asperities. Furthermore, the fracture must be "thin", in the sense that the aperture is small relative to other characteristic length scales in the

problem, such as the distance between asperities:

$$\frac{h}{L} \ll 1 . \tag{6}$$

The first condition (5) holds in most situations of geological importance, although condition (6) may not always be true. An analysis of the effect of a finite value of h/L, which leads to the consideration of viscous drag along the *sides* of the asperities, has been given by Kumar et al. (1989).

If there were no asperities to obstruct the flow, the velocity profile for flow between smooth parallel walls would be parabolic. The velocity vector would be parallel to the pressure gradient, although pointing in the opposite direction, since fluid flows in the direction of *decreasing* pressure. This situation leads to the well-known result $Q = h^3|\nabla P|/12\mu$ (Schlichting 1968), often known as the "cubic law". The presence of the asperities, however, causes the fluid to follow a tortuous path, and the above-discussed solution will not hold. If conditions (5) and (6) are met, we then make the assumption that the the velocity profile is still parabolic and proportional to the pressure gradient, but that the magnitude and direction of the pressure gradient may vary from point to point:

$$\vec{u} = \frac{-\nabla P}{2\mu} z(z-h) , \tag{7}$$

where z is measured from the bottom face of the fracture. If this velocity distribution is integrated across the thickness of the flow channel, we find that the cubic law $Q = h^3|\nabla P|/12\mu$ holds locally at each point.

Both the pressure gradient and the velocity vector will vary from point to point in the plane of the fracture, the x–y plane. If the velocity profile (7) is plugged into the full Navier-Stokes equations, and use is made of conditions (5) and (6), the result is that the pressure field must satisfy Laplace's equation (Schlichting 1968):

$$\nabla^2 P(x,y) = 0 . \tag{8}$$

This equation must be satisfied throughout those portions of the x–y plane that are not occupied by contact area. Boundary conditions must be prescribed along the entire boundary of the flow field, which includes the outer boundaries as well as the boundaries of the contact areas. The outer boundary will typically consist of a combination of regions of constant pressure, and impermeable regions, along which the normal component of the velocity must vanish. Since the velocity is proportional to the gradient of the pressure, the normal derivative of the pressure must vanish along these portions of the boundary, i.e., $\partial P/\partial n = 0$, where n is the outward unit normal to the boundary, in the x–y plane. Since fluid cannot penetrate into the contact areas, the boundaries of the contact areas are also no-flow boundaries.

The boundary element solution to the flow problem utilizes the fundamental solution to Laplace's equation in two dimensions, which is (Brebbia 1978)

$$G(x,y;\zeta,\eta) = \frac{1}{4\pi}\ln\left[(x-\zeta)^2+(y-\eta)^2\right] , \tag{9}$$

where $G(x,y;\zeta,\eta)$ is the potential at (x,y) due to a point source at (ζ,η). The principal idea behind the boundary element method is that the solution throughout the flow region can be written in terms of point sources of variable magnitude, distributed along the boundary of the flow region. If the boundary is discretized into a finite number of elements, and the potential is assumed to be constant over each element, this leads to a finite number of algebraic equations for the magnitudes of the point sources. A schematic diagram of a typical flow region, containing two contact regions, is shown in Fig. 1. Both the external and internal boundaries are discretized. In our calculations, we take the fracture to occupy a square region in the x–y plane, with two opposing faces being boundaries of constant pressure. The pressure difference between these two faces can be taken as being of unit magnitude. The two other opposing faces are taken to be no-flow boundaries. After solving for the pressure field throughout the flow region, the flux out of the flow region is found by calculating $\partial P/\partial n$ along one of the constant-pressure boundaries, and summing the contribution from each element. Note that while the elasticity equations were solved in the three-dimensional region bounded by the fracture "plane", the flow equations are solved in the two-dimensional region of the fracture plane; hence different discretizations must

be used for the two problems.

4. METHOD OF ANALYSIS

We start our analysis by first generating an aperture distribution, which represents the fracture under zero normal load. These distributions can be quantified by c, the amount of contact area, $\bar{h}$, the mean aperture, σ, the standard deviation of the distributions of apertures, and λ, which measures the correlation between contact area and open area (Coakley 1989). Larger values of λ correspond to more "dispersed" contact areas, while smaller values of λ correspond to contact areas that are more "compact". The hydraulic conductivity of the fracture is computed by the boundary element method, assuming that the aperture is everywhere equal to $\bar{h}$. An increment of normal stress is then applied to the fracture, and its deformation is calculated by the elastostatic boundary element method. In those regions where the fracture is open, the two faces of the fracture move closer together; in some locations the aperture merely decreases, while at other points the deformation may be large enough to create new contact area. After this deformation is found, the contact area and the average aperture are recalculated. The permeability of the new fracture geometry is then calculated, and the process is continued. We thereby generate a relationship between normal stress, the amount of contact area, the average aperture, the normal stiffness, and the permeability. Since each calculation with specified statistical parameters represents one realization of a stochastic process, the procedure is repeated for a number of realizations, in order to arrive at statistically meaningful properties.

5. RESULTS

To illustrate the sort of results that we find with our method, we will examine in detail the stiffness and permeability found for two particular realizations of a simulated fracture. Two such sets of results will be sufficient to illustrate which properties display a strong "sample-to-sample" variance, and which do not. The initial contact area of these two fractures at zero load is 5%, their mean aperture is 10 μm, and the standard deviation of their apertures is 4.756 μm. The λ parameter is taken to be 0.75. At zero stress, the contact area for one of the realizations appears as in Fig. 2, which is to say as a few isolated, slightly irregular patches. As the normal load on the fracture is increased, the percentage of contact area increases at a nearly linear rate (see

Figs. 2 and 3). As is typical of a real fracture, the average joint closure increases with stress, but at a continually decreasing rate (Fig. 4). In other words, the fracture becomes stiffer as the stress increases. This is shown in Fig. 5, where the fracture stiffness is plotted as a function of the normal stress.

As mentioned above, the flow calculations are carried out using the simplification that the aperture is everywhere equal to its average value, $\bar{h}$. This assumption creates an error whose magnitude is difficult to estimate; simulations aimed at bounding this error are currently underway. Since the flow rate, under a fixed pressure gradient, is proportional to the cube of $\bar{h}$, and since $\bar{h}$ decreases rapidly with stress (Fig. 4), we expect that the flow rate will drop off rapidly with stress. This is verified in Fig. 6, which shows the flow rate initially dropping off at a rate roughly proportional to the 3rd power of the stress, and then dropping off more rapidly after the stress reaches some "critical" value. This rapid falloff may correspond to the percolation limit, at which a connected open pathway for fluid flow no longer exists. Another instructive way to look at the results is as in Fig. 7, which shows the flow rate, normalized to its zero-stress value, plotted as a function of the average aperture. Note that as the stress increases, the flowrate falls below that which would be predicted by the cubic law. This reflects the "tortuosity" effect, in which the fluid is forced to flow around the closed-off asperity regions. As described by the models of Walsh (1981) and Chen et al. (1989), the tortuosity is an increasing function of contact area, hence it is to be expected that the tortuosity will increase as the stress increases.

For the same set of statistical parameters, there is of course some variation in the calculated properties of the fracture, between different realizations. Fractures with different initial aperture distributions, but the same mean, standard deviation, and initial contact area, tend to have very nearly the same mechanical behavior (see Figs. 3-5). The hydraulic properties, on the other hand, show much more variability (Figs. 6,7). At stresses below about 30 MPa, the permeability-pressure curves for the different realizations lie close together. However, the pressure above which the permeability drops off rapidly to zero varies from about 40 MPa to 70 MPa between the different fracture realizations.

The hydromechanical behavior of the fractures also depends on the statistical parameter λ. Recall that larger values of λ correspond to contact areas that are more

dispersed, while smaller values of λ correspond to more compact regions of contact. For a given amount of contact area, the stiffness is an increasing function of λ, reflecting the fact that, for example, two separate contact areas of 1 mm^2 will be "stiffer" than one contact region of 2 mm^2, which is certainly plausible. The effect of λ on the flow properties is more complicated, and implicit, since the distribution of aperture directly affects the mechanical closure of the fracture, which in turn explicitly determines the permeability. Detailed examples of the effect of λ on the hydromechanical properties can be found in the thesis by Chen (1990).

6. CONCLUSIONS

Boundary element methods have been used to study the deformation and permeability of simulated fractures as a function of normal stress. The fractures are statistically characterized by their initial mean aperture, aperture standard deviation, and a parameter that quantifies the compactness of the contact regions. Many of the observed features of real rock fracture behavior are reproduced by these simulations. The stiffness of the fractures drops off asymptotically as the stress is increased, while the contact area increases at a nearly linear rate. At low stresses, the permeability drops off at a rate proportional to the third power of the normal stress (cf., Walsh 1981). At some critical stress, typically on the order of 30-70 MPa, the percolation limit is reached, at which a connected pathway for fluid flow no longer exists, and the permeability drops precipitously. For given values of the statistical parameters that characterize the fracture, the critical stress is the only property that exhibits a strong sample-to-sample variation. The possibility now exists of simulating the mechanical and hydraulic behavior of real fractures, based on measured aperture distributions. and comparing the predictions with experimental results.

ACKNOWLEDGEMENTS

This work was supported by the Office of Civilian Radioactive Waste Management under the Repository Technology and Transportation Division, and by the Director, Office of Basic Energy Sciences, U.S. Department of Energy, under Contract No. DE-AC03-76SF00098.

REFERENCES

Barton, N., S. Bandis & K. Bakhtar. 1985. Strength, deformation and conductivity coupling of rock joints. Int. J. Rock Mech. Min. Sci. & Geomech. Abstr. 22:121-140

Batchelor, G.K. 1967. Introduction to fluid dynamics. Cambridge: Cambridge University Press.

Brebbia, C.A. 1978. The boundary element method for engineers. London: Pentech Press.

Brown, S.R. 1987. Fluid flow through rock joints: the effect of surface roughness. J. Geophys. Res. 92:1337-1347.

Brown, S.R. & C.H. Scholz 1985. Closure of random elastic surfaces in contact. J. Geophys. Res. 90:5531-5545.

Chen, D.W. 1990. Coupled stiffness-permeability analysis of a single rough-surfaced fracture by the three-dimensional boundary element method. Ph.D. thesis, University of California at Berkeley.

Chen, D.W., R.W. Zimmerman & N.G.W. Cook. 1989. The effect of contact area on the permeability of fractures. In A.W. Khair, (ed.), Proceedings of the 30th U.S. Symposium on Rock Mechanics, p. 81-88. Rotterdam: Balkema.

Coakley, K. 1989. Spatial statistics for predicting flow through a single fracture. Ph.D. thesis, Stanford University.

Crouch, S.L. & A.M. Starfield. 1983. Boundary element methods in solid mechanics London: Allen & Unwin.

Hopkins, D.L., N.G.W. Cook & L.R. Myer. 1987. Fracture stiffness and aperture as a function of applied stress and contact geometry. In I.W. Farmer et al. (eds.), Proc. 28th U.S. Symp. Rock Mech., p. 673-680.

Kumar, S., R.W. Zimmerman & G.S. Bodvarsson. 1989. Permeability of a fracture with cylindrical asperities. Report LBL-27626, Lawrence Berkeley Laboratory.

Pyrak-Nolte, L.J., L.R. Myer, N.G.W. Cook & P.A. Witherspoon. 1987. Hydraulic and mechanical properties of natural fractures in low permeability rock. In G. Herget & S. Vongpaisal (eds.), Proc. 6th Int. Cong. Rock Mech., p. 224-231. Rotterdam: Balkema.

Rongved, L. 1957. Dislocation over a bounded plane area in an infinite solid. J. Appl. Mech. 24:252-254.

Schlichting, H. 1968. Boundary-layer theory, 6th ed. New York: McGraw-Hill.

Sokolnikoff, I.S. 1956. Mathematical theory of elasticity, 2nd ed. New York: McGraw-Hill.

Tsang. Y.W. & P.A. Witherspoon. 1981. Hydromechanical behavior of a deformable rock fracture subject to normal stress. J. Geophys. Res. 86:9287-9298.

Walsh, J.B. 1981. The effect of pore pressure and confining pressure on fracture permeability. Int. J. Rock Mech. Min. Sci. & Geomech. Abstr. 18:429-435.

Zimmerman, R.W., M.S. King & W.H. Somerton. 1986. Compressibility of porous rocks. J. Geophys. Res. 91:12765-12778.

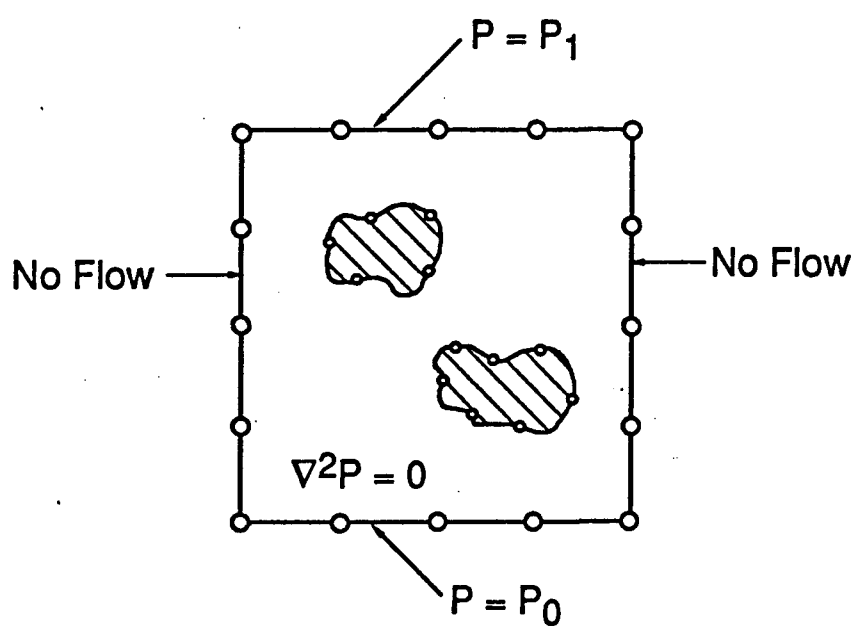

Fig. 1. Schematic diagram of flow region, showing two asperities, the constant-pressure and no-flow boundary conditions, and the boundary discretization.

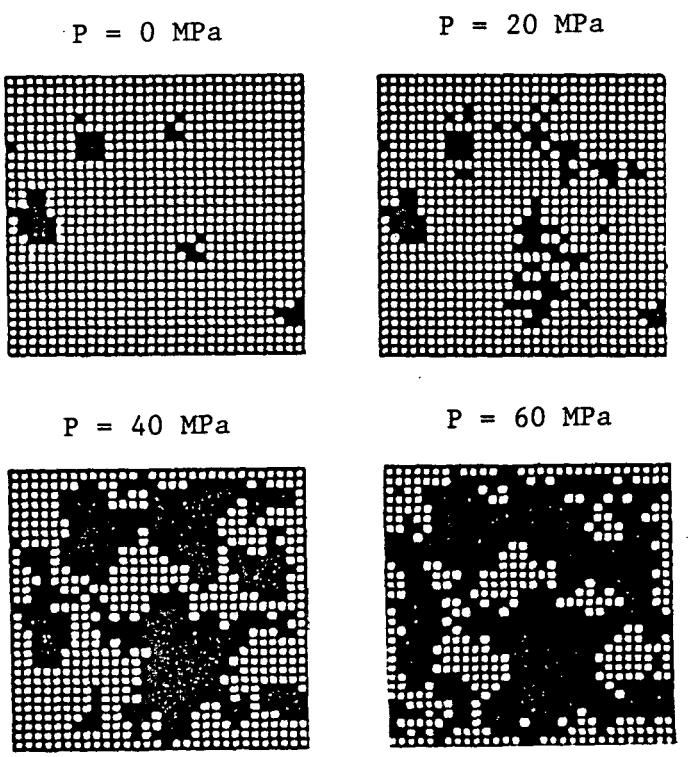

Fig. 2. Contact area (in black) as a function of normal stress. Note the lack of a connected (top-to-bottom) flow path at 60 MPa.

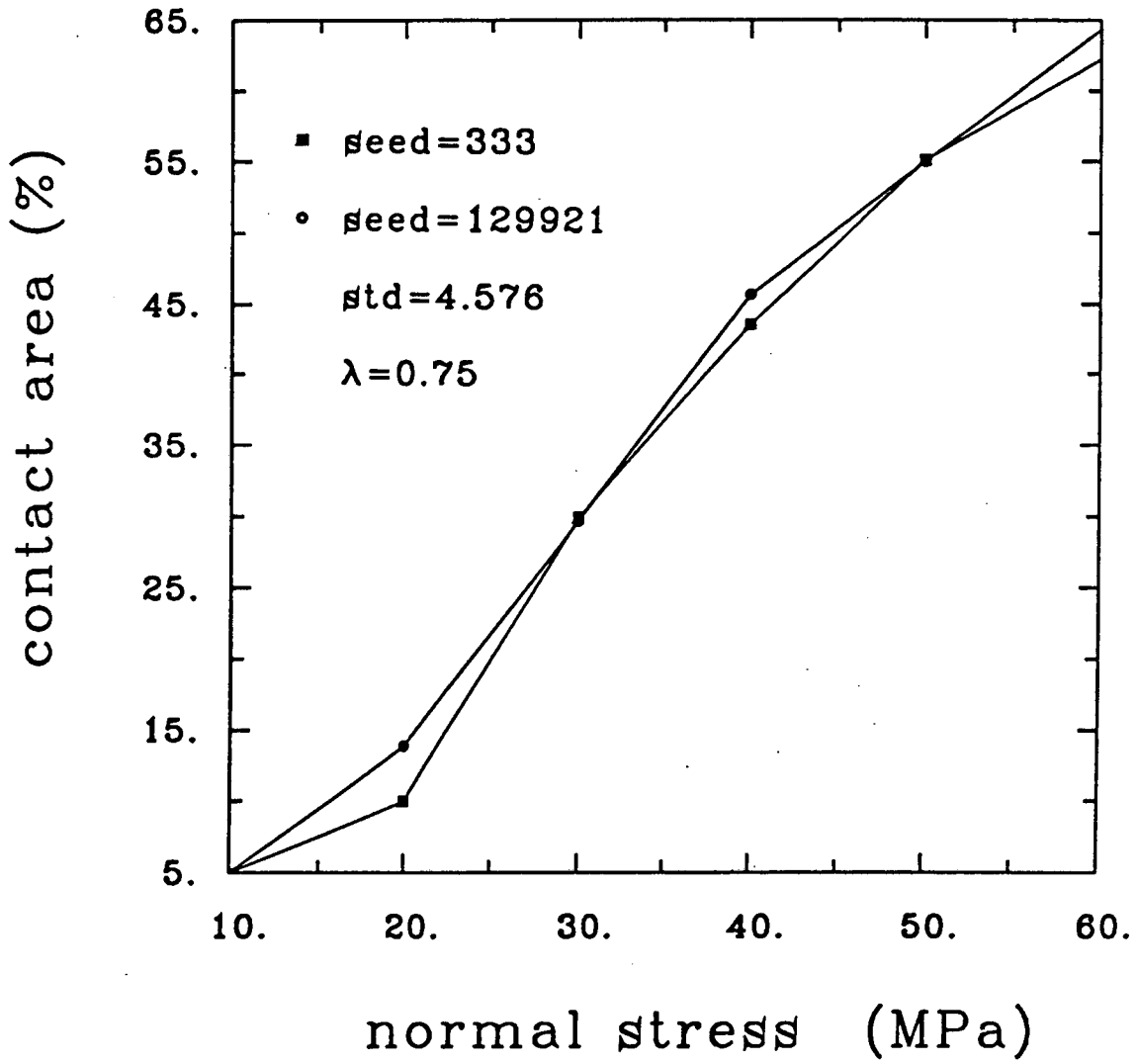

Fig. 3. Percent contact area as a function of normal stress, for two different realizations.

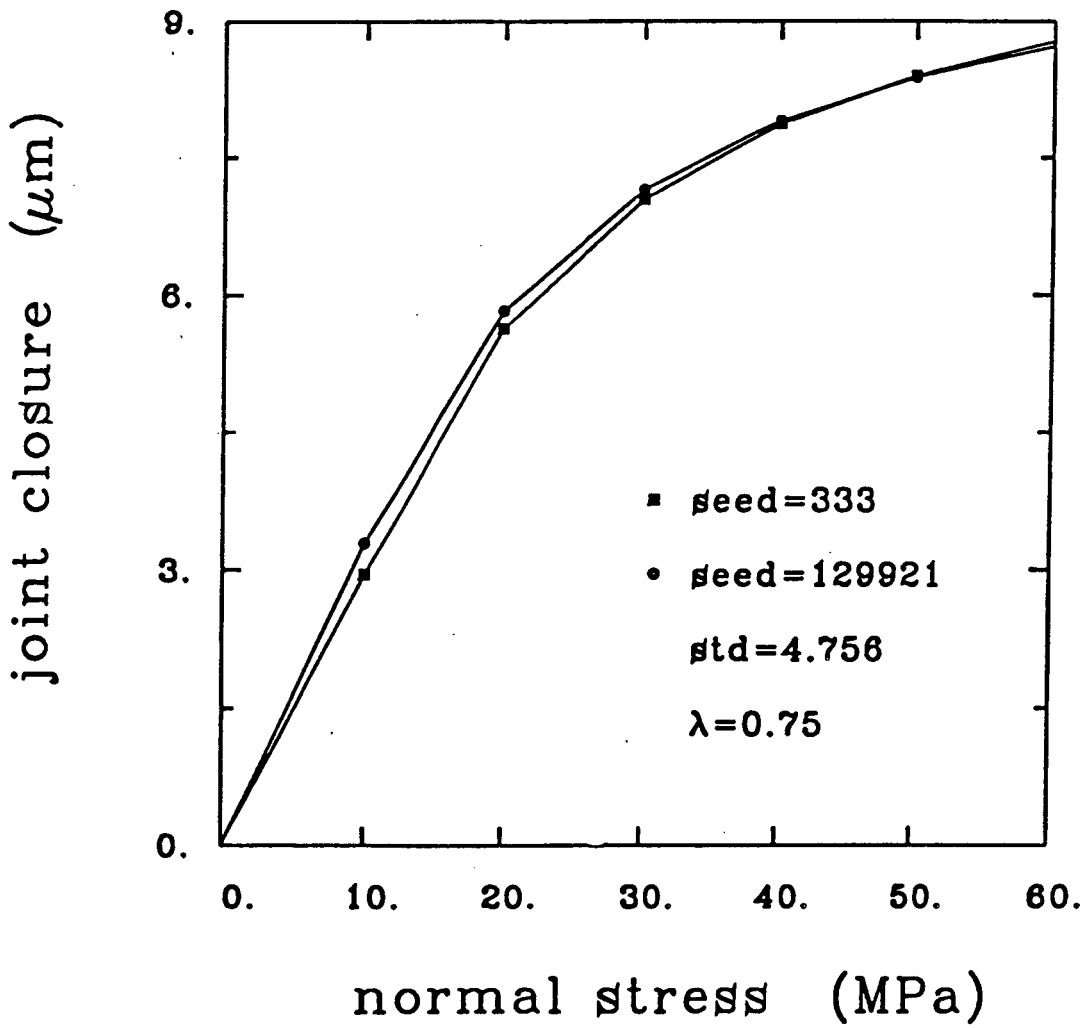

Fig. 4. Joint closure as a function of normal stress, for two different realizations.

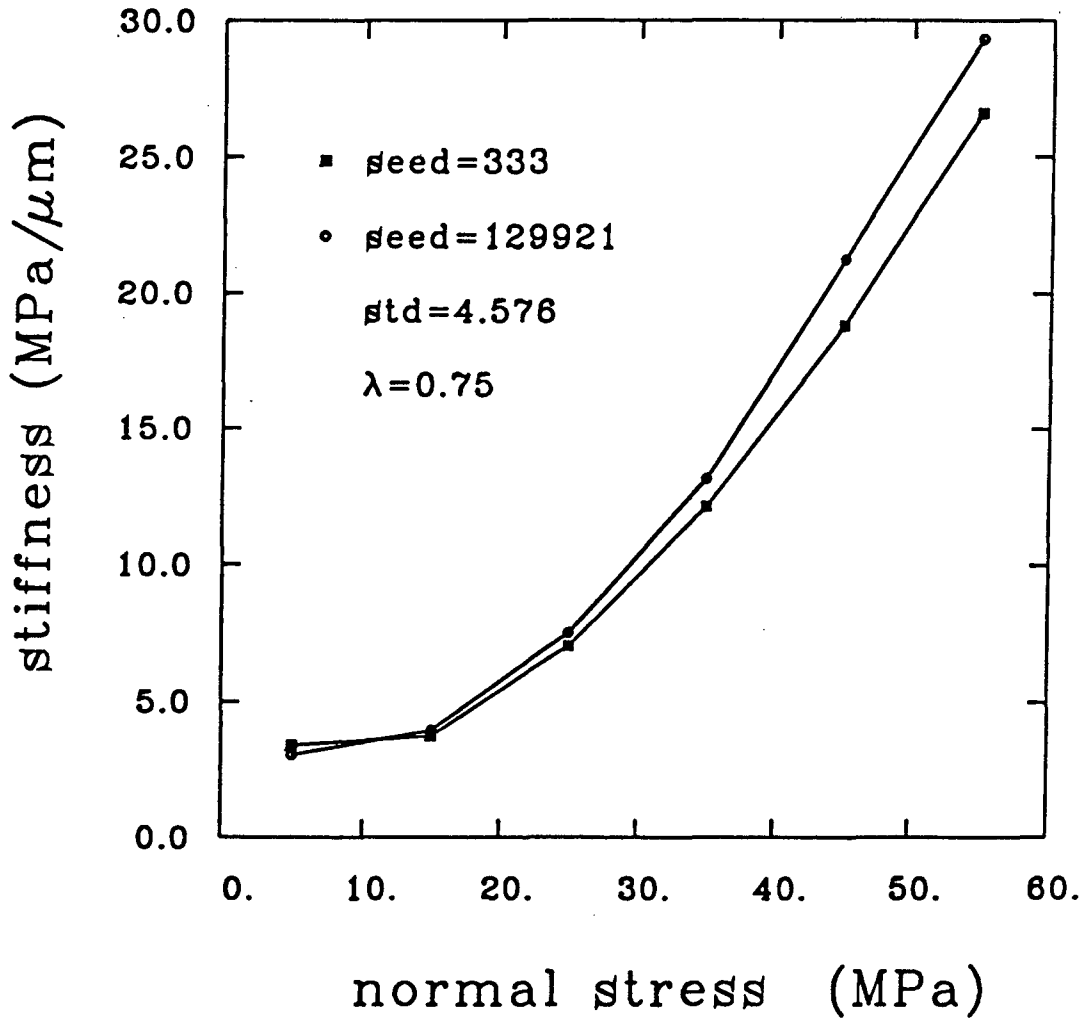

Fig. 5. Stiffness as a function of normal stress, for two different realizations.

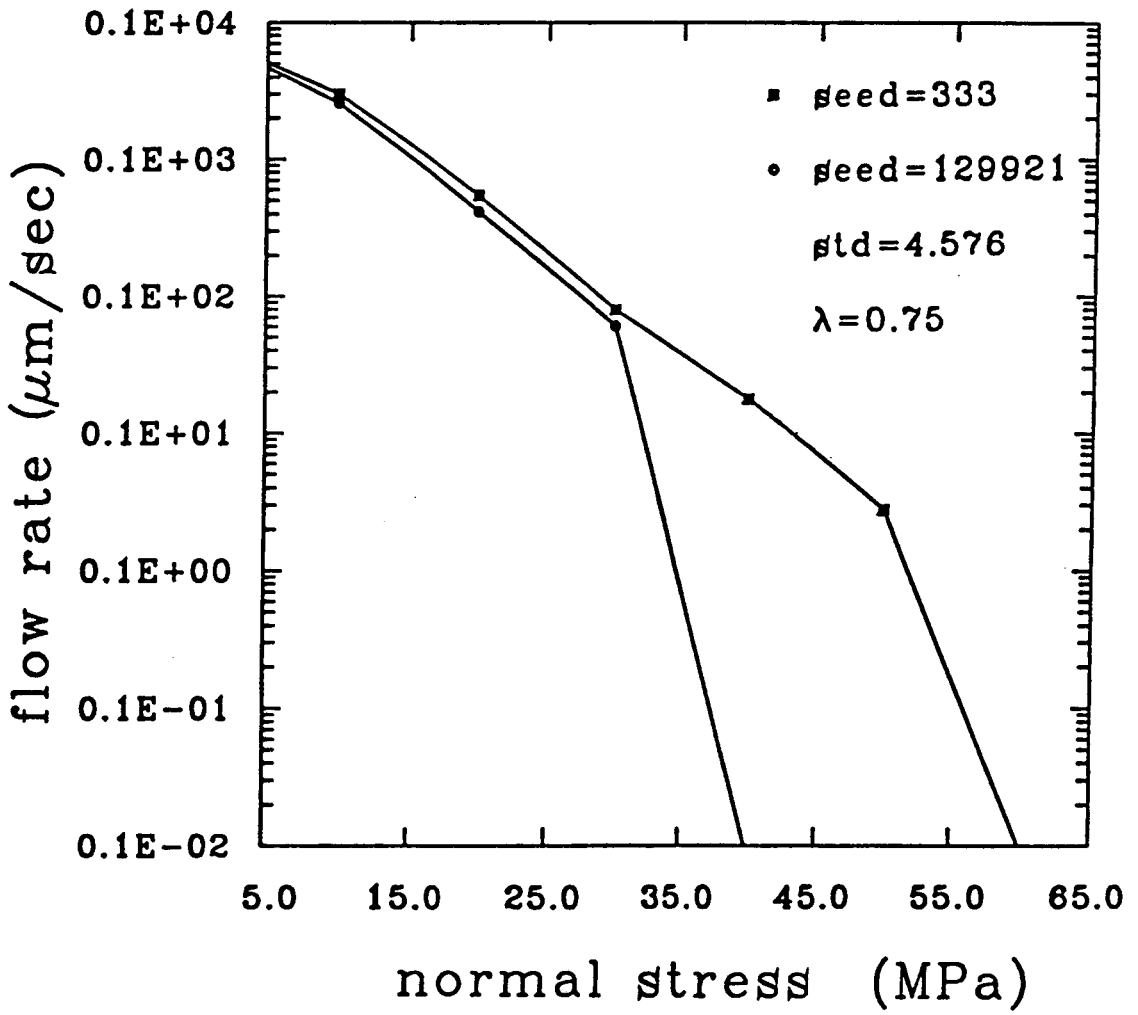

Fig. 6. Flow rate under a unit pressure gradient, as a function of normal stress,

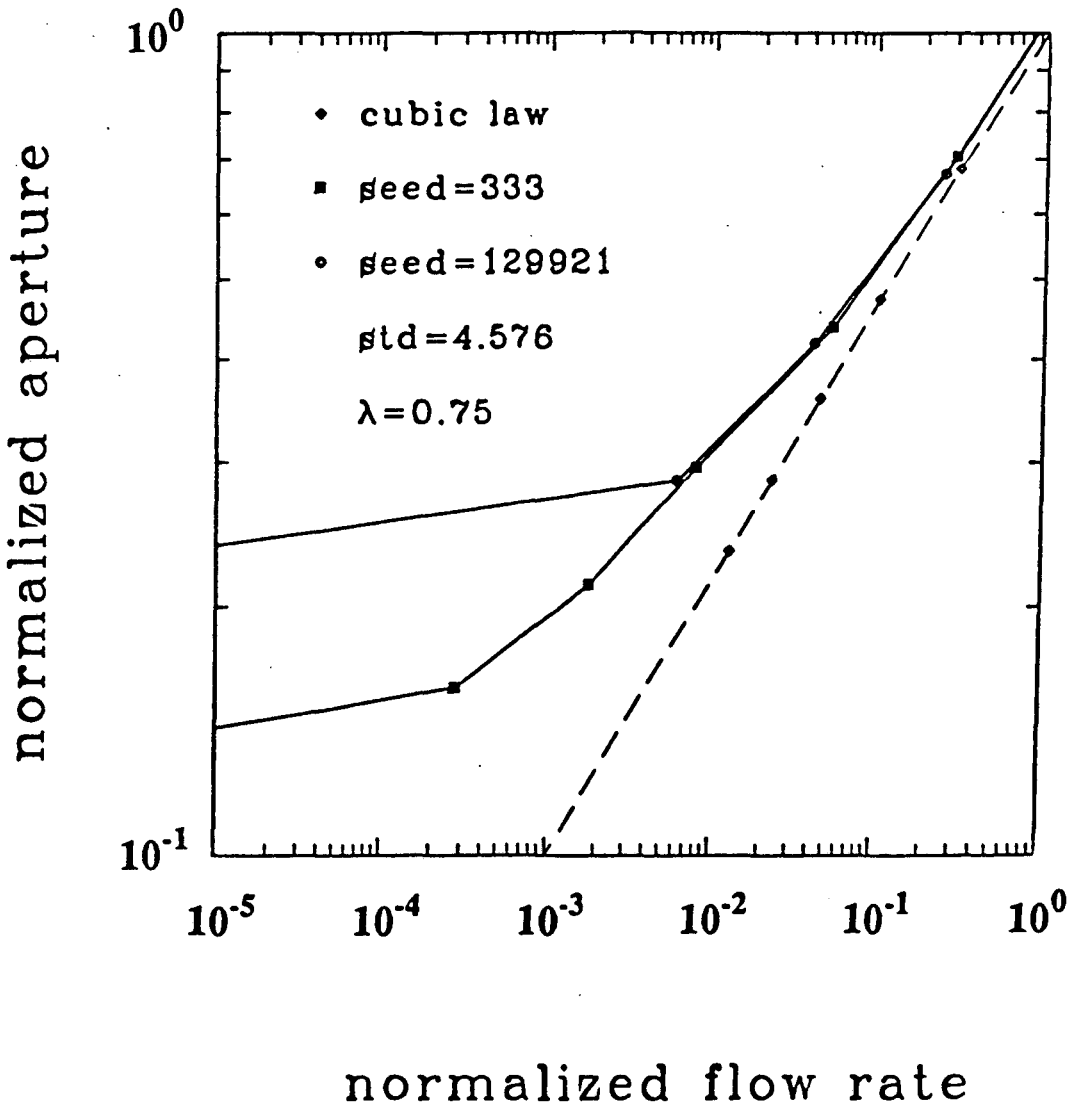

Fig. 7. Permeability as a function of mean aperture for two realizations, and comparison with the "cubic law".

LAWRENCE BERKELEY LABORATORY
TECHNICAL INFORMATION DEPARTMENT
1 CYCLOTRON ROAD
BERKELEY, CALIFORNIA 94720